Hydrogen bonding and proton transfer in small hydroxylammonium nitrate clusters: A theoretical study

ARTICLE *in* THE JOURNAL OF CHEMICAL PHYSICS · AUGUST 2003

Impact Factor: 2.95 · DOI: 10.1063/1.1593011

Hydrogen bonding and proton transfer in small hydroxylammonium nitrate clusters: A theoretical study

Saman Alavi and Donald L. Thompson[a)]
Department of Chemistry, Oklahoma State University, Stillwater, Oklahoma 74078

(Received 31 March 2003; accepted 29 May 2003)

Structures and energies of gas-phase hydroxylammonium nitrate (HAN), $HONH_3NO_3$, are determined using density functional theory and the 6-311++G(d,p) basis set. Three stable configurations are found for HAN which involve strong hydrogen bonding between hydroxylamine and nitric acid molecules. In the most stable configuration, both the oxygen and the nitrogen of hydroxylamine are hydrogen bonded to sites on the nitric acid molecule. In the less stable HAN structures only the oxygen or the nitrogen of hydroxylamine are hydrogen bonded. Two stable structures for the $(HAN)_2$ complex are investigated. The more stable structure is ionic, with the nitric acid proton having transferred to the nitrogen of hydroxylamine. Strong electrostatic and hydrogen-bonding interactions stabilize this structure. The other stable form of $(HAN)_2$ has fewer hydrogen bonds and is composed of interacting neutral nitric acid and hydroxylamine molecules. Binding energies are determined for all structures along with corrections for basis set superposition errors in the HAN molecules. Proton exchange reaction paths are studied for the HAN configurations. The saddle points for the proton exchange process are ionic forms of HAN with interacting $HONH_3^+$ and NO_3^- moieties. These ionic structures are 13.5 and 13.6 kcal/mol higher in energy than the neutral hydrogen-bonded complexs of $HONH_2$ and HNO_3 from which they are formed. The electrostatic attractions between the ions are sufficient to stabilize the ionic form of $(HAN)_2$, whereas in the HAN ''monomer'' the interaction energy for single $HONH_3^+$ and NO_3^- ions is not sufficient to compensate for the energy required for proton transfer from nitric acid to the hydroxylamine group. A correlation based on the bond-valence theory which describes the bond lengths of the hydrogen bonds is examined for the complexes. All the hydrogen bonds follow the correlation well. © *2003 American Institute of Physics.* [DOI: 10.1063/1.1593011]

I. INTRODUCTION

Hydrogen bonding has a significant effect on the structural properties of ammonium salts, and proton transfer plays a crucial role in their chemistry. There is evidence that physical changes during the chemical decomposition of these salts are often precursory to or concurrent with the chemical reactions. These physical changes of state often involve proton transfer. For example, the orthorhombic to cubic crystalline phase transition in ammonium perchlorate at 240 °C results in the free rotation of the perchlorate ions in the solid and leads to proton transfer.[1] Ammonium nitrate also undergoes three solid-state phase transformations above 298 K and decomposition of the solid only becomes extensive at temperatures above 440 K, which is the melting point of ammonium nitrate.[2,3] Mass spectrometric studies show that the first stage of this decomposition reaction is the transformation of the ionic ammonium nitrate into the acid and base, HNO_3 and NH_3, respectively.[4] Similarly, the decomposition of ammonium dinitramide (ADN) at high temperatures may be initiated by the sublimation of the ADN molecules, which involves a proton transfer from ammonium to the dinitramide ion.[4] Proton transfer in the gas phase plays an important role in the ADN decomposition reaction.[5]

We are interested in the atomic-level mechanisms for the decomposition of nitrate and dinitramide salts as functions of temperature and pressure. A variety of theoretical methods are being used to explore the fundamental properties and elementary processes in these salts. We want to understand how hydrogen bonding and proton transfer affect the crystal structures, the transitions between crystal phases, the changes in physical state (i.e., melting and vaporization), and the chemical reactions that can occur between ion pairs and acid–base pairs. Force fields that describe the crystal phases of ammonium nitrate and ammonium dinitramide have been developed.[3,6] We have used the ADN potential to study the influence of temperature and pressure on its physical properties, including melting.[7,8] We have also used *ab initio* and density functional theory (DFT) calculations to investigate proton transfer in clusters of these salts to gain some insight into the interconversion between ion pairs and acid–base pairs.[9,10] The calculations predict that in the gas phase, single molecules of ammonium nitrate and ammonium dinitramide consist of hydrogen-bonded neutral units, $[H_3N\cdots HONO_2]$ and $[H_3N\cdots HN(NO_2)_2]$, respectively. However, the stable configurations of clusters of two molecules in the gas phase consist of hydrogen-bonded ion pairs, $[H_3NH^+\cdots{}^-ONO_2]_2$ and $[H_3NH^+\cdots{}^-N(NO_2)_2]_2$. Since it appears that much of the chemistry involves gas-phase acid and base molecules, we have used the same methods to investigate the energetics

a)Electronic mail: dlt@okstate.edu

and pathways for the unimolecular decomposition of ammonium dinitramide in the gas phase.[5] The computed results predict that the activation barriers to the first stage of the dinitramide decomposition depend strongly on the protonated state of the dinitramide moiety.

In the present study, we have used DFT calculations to investigate hydrogen bonding and proton transfer in gas-phase hydroxylammonium nitrate (HAN), $(HONH_2)HNO_3$. The structures and energetics of HAN monomers and dimers were investigated. Solid HAN is ionic, with the ''nitric acid proton'' residing on the nitrogen of hydroxylamine and with all hydrogen atoms involved in hydrogen bonding. Compared to other ammonium and substituted ammonium salts,[11] the hydroxylamine molecule has the interesting aspect that it includes two hydrogen bonding functional groups, the OH which is a stronger proton donor site and the NH_2 which is the stronger hydrogen-bonding proton acceptor site.[12,13] The presence of these two groups allows for O···HO, N···HO, and O···HN hydrogen bonding and two proton transfer pathways in HAN.

The solid-state structure of HAN and its per-deuterated homolog have been determined by x-ray crystallography.[14] The unit cell of solid HAN is monoclinic, with four molecules per unit cell. The solid state and aqueous solution infrared (IR) vibrational spectra of HAN have been obtained and interpreted.[15] Klein[16] has developed a three-stage combustion mechanism for HAN, the first stage of which is proton transfer in the condensed phase to produce $HONH_2$ and HNO_3. The decomposition reaction of HAN begins at 130 °C and some of the initial stages of reaction may begin in the gas phase. Concentrated aqueous solutions and solid-state samples of HAN are combustible and can be used as an alternative oxidant to NH_4ClO_4 in propellant fuels.[17]

In Sec. II, the theoretical methods used to study the structure and energetics of the HAN and $(HAN)_2$ molecules are described. The results of the study are given Sec. III, which is followed by a discussion, Sec. IV. The article ends with a summary in Sec. V.

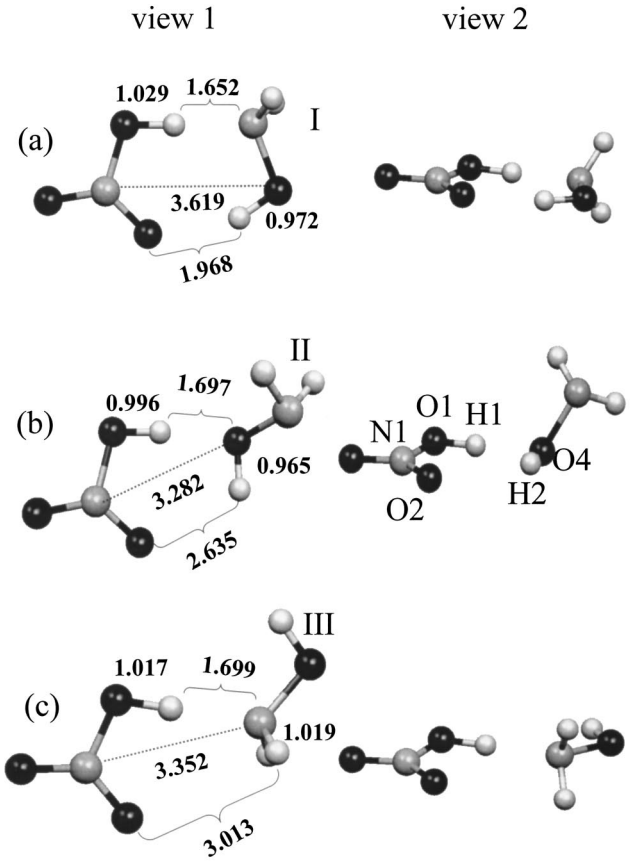

FIG. 1. The three stable configurations of the hydroxylamine nitrate molecule. The energies, geometrical parameters, and vibrational frequencies of these structures are given in Tables I and II. Selected bond lengths (Å) are shown in the figure. (a) Two views of structure I, the lower energy hydrogen-bonded configuration for hydroxylamine. View 2 is rotated by approximately 90° with respect to view 1. (b) Two views of structure HAN II configuration where only the OH end of hydroxylamine participates in hydrogen bonding. View 2 is rotated by approximately 90° with respect to view 1. (c) Two views of structure HAN III configuration where only the NH_2 end of hydroxylamine participates in hydrogen bonding. View 2 is rotated by approximately 90° with respect to view 1. The atoms shown in black are oxygen, those in gray are nitrogen, and those in light gray are hydrogen. The numbering scheme for the atoms is shown in (b).

II. THEORETICAL METHODS

Calculations were performed with the GAUSSIAN 98[18] suite of programs at the density functional theory (DFT) level using the B3LYP hybrid Hartree–Fock nonlocal approach of Becke[19] with the 6-311++G(d,p) basis set. The geometries and vibrational frequencies of HAN and $(HAN)_2$ cluster at this level of theory are considered accurate.[20] Geometric optimization without symmetry constraints were performed to obtain minimum energy structures which were verified by vibrational frequency analysis. Harmonic frequencies were calculated with analytical force constants, and nonscaled values of the frequencies are used for determining zero-point energies. The basis set superposition error (BSSE)[20–22] for the binding energies of the HAN clusters was estimated using the counterpoise method[22,23] along with corrections for the relaxation energies of the nitric acid and hydroxylamine fragments.[24]

III. RESULTS

We have found three stable structures for isolated HAN molecules, which are labeled as I, II, and III in Fig. 1, and investigated two stable structures for the dimer, $(HAN)_2$, which are labeled as IV and V in Fig. 2. Two views of HAN and $(HAN)_2$, the second view rotated by about 90° with respect to the first, are shown in these figures. All three HAN structures are hydrogen bonded and do not show proton transfer from nitric acid to hydroxylamine. The most stable form of $(HAN)_2$ is the ionic structure IV. Ionic $(HAN)_2$ has C_2 symmetry and three of the four protons on the $HONH_3^+$ ions participate in hydrogen bonding. The $(HAN)_2$ structure V is not ionic and has C_i symmetry. In this dimer form, two of the three hydroxylamine protons participate in hydrogen bonding.

The structural parameters and energies of isolated gas-phase hydroxylamine and nitric acid calculated at the B3LYP/6-311++G(d,p) level are compared with experi-

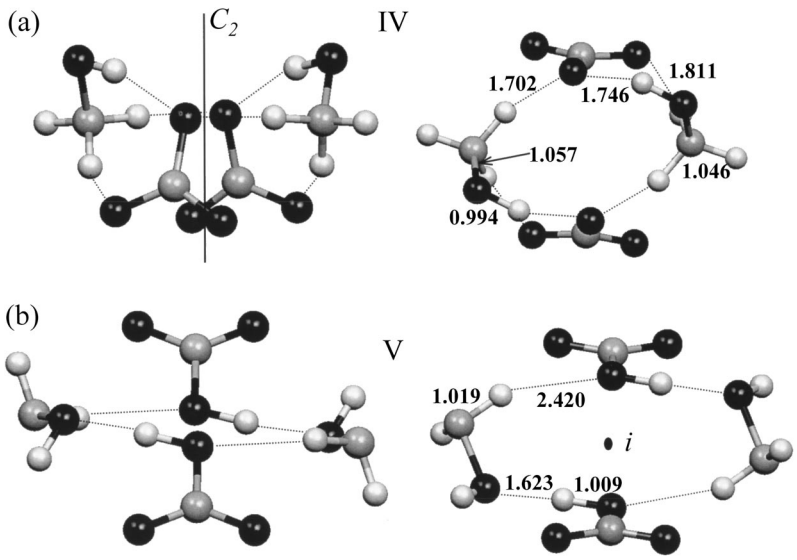

FIG. 2. The structure of two gas-phase HAN dimers. The lengths of hydrogen bonds (Å) are shown in the figure. (a) Configuration IV consists of interacting ions, where three of the four hydrogen atoms of $HONH_3^+$ participate in hydrogen bonding. This structure has C_2 symmetry and is shown in two views. (b) The hydrogen-bonded configuration V shown in two views. This structure has C_i symmetry and does not show proton transfer between the hydroxylamine and nitric acid units.

mental results in Table I. The labeling scheme for the atoms used in Table I is shown in Fig. 1. The deviation from experiment of the calculated bond lengths in both species is less than 1%, and the maximum deviation in the calculated bond angles is 1.4%. Structural parameters of the hydroxylamine and nitric acid components of HAN I, HAN II, and HAN III are also given in Table I. In this table, significant changes are seen in the bond lengths and bond angles of the protons involved in hydrogen bonding, when going from isolated hydroxylamine and nitric acid molecules to HAN complexes.

In Table II the calculated harmonic vibrational frequencies of isolated hydroxylamine and nitric acid are compared with experimental results. The symmetry labels of the vibrations along with a description of each vibration are also given. The unscaled calculated frequencies show good agreement with the experimental values. The vibrational frequencies of the hydroxylamine and nitric acid moieties of the HAN I, HAN II, and HAN III are given in the last two columns of Table II. Some large frequency shifts and intensity enhancements are observed in going from the isolated $HONH_2$ and HNO_3 molecules to the hydrogen-bonded HAN structures. A large frequency shift is seen in the $\nu_1(a')$ O–H stretch frequencies of $HONH_2$ in HAN I, which shifts to 3684 cm^{-1} from the value of 3823 cm^{-1} in isolated $HONH_2$. The HONO torsional vibration of HNO_3 in HAN I (1092 cm^{-1}), HAN II (811 cm^{-1}), and HAN III (1026 cm^{-1}) shows significant shifts relative to the HONO torsional vibration of isolated HNO_3 (461 cm^{-1}).

The absolute energies and binding energies of HAN I, II,

TABLE I. Experimental and calculated equilibrium bond lengths (Å), bond angles (degrees), and total energies (hartrees) of $HONH_2$ and HNO_3 in the gas phase and in HAN.

Molecule	Parameter	Experiment on isolated molecule	Calculated[a]			
			Isolated molecule	HAN I[b]	HAN II[b]	HAN III[b]
$HONH_2(C_s)$[c]	r(OH)	0.963	0.963	0.972	0.965	0.964
	r(NO)	1.453	1.445	1.430	1.442	1.434
	r(NH)	1.016	1.019	1.019	1.018	1.019
	∠NOH	101.4	102.8	102.8	104.8	104.2
	∠HNH	107.1	106.2	106.7	106.9	106.2
	∠HNO	103.2	104.2	105.5	103.9	105.2
	E[d]		−131.766 887 (25.3)			
$HNO_3(C_s)$[e]	r(O1H)	0.964	0.972	1.029	0.996	1.017
	r(NO1)	1.406	1.416	1.367	1.387	1.380
	r(NO2)	1.211	1.210	1.229	1.218	1.221
	r(NO3)	1.199	1.194	1.199	1.199	1.200
	∠HON	102.2	103.6	107.1	105.0	105.4
	∠O1NO2	115.9	115.8	117.2	116.6	116.6
	∠O1NO3	113.9	113.8	115.7	114.8	115.2
	E[d]		−280.978 606 (16.5)			

[a]B3LYP/6-311++G(d,p) level.
[b]Structures are given in Fig. 1.
[c]Experimental data from Luckhaus, Ref. 13.
[d]Zero-point energy (kcal/mol) is given in parentheses.
[e]Experimental data from Cox and Riveros, Ref. 28.

TABLE II. Experimental and calculated harmonic frequencies (cm^{-1}) and infrared intensities (km/mol) of $HONH_2$ and HNO_3.

Label[a]	Description	Experiment on isolated molecule	Calculated			
			Isolated molecule	HAN I	HAN II	HAN III
			$HONH_2$[b]			
$\nu_1(a')$	OH stretch	3650	3823(46)	3684(355)	3810(88)	3810(49)
$\nu_2(a')$	NH stretch	3294	3445(2)	3447(1)	3454(0)	3454(3)
$\nu_3(a')$	HNH bend	1604	1672(21)	1665(32)	1673(40)	1664(10)
$\nu_4(a')$	NOH bend	1353	1389(29)	1487(51)	1367(60)	1420(32)
$\nu_5(a')$	NH_2 wag	1115	1135(132)	1191(144)	1146(175)	1184(114)
$\nu_6(a')$	NO stretch	895	925(15)	983(0)	927(125)	976(29)
$\nu_7(a'')$	NH stretch	3359	3525(2)	3518(13)	3541(6)	3525(17)
$\nu_8(a'')$	NH_2 twist	1294	1328(0)	1320(1)	1343(24)	1321(18)
$\nu_9(a'')$	OH torsion	386	445(198)	554(110)	507(156)	424(70)
			HNO_3[c]			
$\nu_1(a')$	OH stretch	3550	3728(102)	2653(2008)	3258(1315)	2864(1962)
$\nu_2(a')$	ONO stretch	1709	1754(435)	1739(191)	1746(331)	1743(254)
$\nu_3(a')$	ONO stretch	1326	1349(319)	1313(301)	1326(187)	1326(316)
$\nu_4(a')$	NOH bend	1304	1312(52)	1532(386)	1485(285)	1522(338)
$\nu_5(a')$	NO stretch	878	897(199)	963(164)	938(72)	942(166)
$\nu_6(a')$	ONO bend	647	649(20)	698(5)	680(4)	686(3)
$\nu_7(a'')$	ONO bend	580	586(7)	655(4)	639(5)	650(7)
$\nu_8(a'')$	N out-of-plane bend	763	774(8)	786(16)	778(64)	788(15)
$\nu_9(a'')$	OH torsion	458	461(138)	1092(106)	811(75)	1026(108)

[a]Mode assignments are for isolated $HONH_2$ and HNO_3 molecules.
[b]Experimental data from Luckhaus, Ref. 13.
[c]Experimental data from Ref. 29.

and III are given in Table III. Basis set superposition errors must be taken into account when determining binding energies.[20–22] The binding energies of the HAN molecules corrected for BSSE are given in Table III. The counterpoise corrections (along with fragment relaxation energies) for the binding energies of HAN I, II, and III are ≈1 kcal/mol. These values are consistent with the magnitudes of the BSSE for ammonium nitrate[25] and ammonium dinitramide[10] molecules. It must be noted that counterpoise calculations for the BSSE from DFT show irregular convergence behavior.[26,27] The HAN structure I has both the hydroxylamine oxygen and nitrogen participating in strong hydrogen bonding with the nitric acid group, and is more strongly bound than structures II and III; the binding energies are 12.7, 8.2, and 10.1 kcal/mol, respectively. The hydroxylamine nitrogen is a stronger proton acceptor in hydrogen bonding than is the oxygen. In structure II (see Fig. 1) the hydroxylamine oxygen, and in structure III the hydroxylamine nitrogen is both the proton donor and acceptor. The proton on nitric acid is more acidic and forms a stronger hydrogen bond than the proton of the OH group of hydroxylamine in HAN II; the lengths of these two OH···O hydrogen bonds are, respectively, 1.697 and 2.635 Å. These lengths give an indication of the strengths of the two hydrogen bonds.

X-ray diffraction studies indicate that in the solid state HAN is ionic. The nitric acid proton has been transferred to the nitrogen of the hydroxylamine.[15] To find the smallest gas-phase HAN cluster for which proton transfer occurs, minimum energy configurations of $(HAN)_2$ clusters were computed. The most stable form of $(HAN)_2$ is ionic [see structure IV in Fig. 2(a)]. Geometric parameters for this

TABLE III. Total energies E (hartrees) along with zero-point energies (kcal/mol), and binding energies D_b (kcal/mol) of the hydrogen-bonded configurations of the HAN molecule along with hydrogen bonded and ionic forms of the $(HAN)_2$ molecule.

Structure[a]	(E)[b]	(D_b^{NCP})[c]	(D_0^{NCP})[c,d]	(D_b^{BSSE})[e]
I-HAN (NO-bonded)	−412.768 518 (43.5)	14.4	12.7	13.2
II-HAN (O-bonded)	−412.760 568 (43.0)	9.4	8.2	8.5
III-HAN (N-bonded)	−412.763 644 (43.0)	11.4	10.1	10.4
IV-$(HAN)_2$ (ionic)	−825.558 000 (89.7)	42.0	35.9	
V-$(HAN)_2$ (molecular)	−825.532 967 (86.8)	26.3	23.1	
VI-HAN (TS1)	−412.735 282 (40.7)	−6.4	−5.3	
VII-HAN (TS2)	−412.746 804 (43.5)	0.8	−0.9	

[a]Roman numerals correspond to structures in Figs. 1 and 2.
[b]Zero-point energy is given in parentheses.
[c]NCP: noncounterpoise calculation.
[d]Includes zero-point energy corrections.
[e]Binding energy corrected for BSSE.

TABLE IV. Equilibrium bond lengths (Å), bond angles (degrees), and total energies (hartrees) of $HONH_3^+$ and NO_3^- in the gas phase and in the ionic form of $(HAN)_2$ from B3LYP calculations with the 6-311++G(d,p) basis set.

Molecule	Parameter	Isolated	Ionic $(HAN)_2$
$HONH_3^+(C_s)$	r(OH)	0.975	0.992
	r(NO)	1.406	1.413
	r(NH)	1.029,1.031,1.031	1.018,1.048,1.058
	∠NOH	107.4	100.6
	∠ONH	104.6,112.4,112.4	107.0,107.7,109.9
	∠HNH	108.4,108.4,110.3	109.3,111.2,111.6
	E	−132.086 514	
$NO_3^-(D_{3h})$	r(NO)	1.260	1.223,1.249,1.304
	∠ONO	120.0	118.0,118.6,123.4
	E	−280.457 550	

TABLE V. Harmonic frequencies (cm^{-1}) and infrared intensities (km/mol) of $HONH_3^+$ and NO_3^- calculated at the B3LYP/6-311++G(d,p) level.

Label[a]	Description	Isolated ion	Ionic $(HAN)_2$[b]
		$HONH_3^+$	
$\nu_1(a')$	OH stretch	3700(154)	3291(263); 3302(1379)
$\nu_2(a')$	NH stretch	3425(158)	3520(10); 3520(189)
$\nu_3(a')$	NH stretch	3327 (30)	2862(21); 2904(1791)
$\nu_4(a')$	HNH bend	1640(41)	1718(40); 1711(105)
$\nu_5(a')$	NH_3 umbrella mode	1592(48)	1631(1); 1570(50)
$\nu_6(a')$	HON bend	1476(50)	1582(68); 1608(17)
$\nu_7(a')$	NH_2 wag	1152(52)	1212(163); 1213(77)
$\nu_8(a')$	NO stretch	1016(16)	1032(18); 1030(47)
$\nu_9(a'')$	NH stretch	3399(125)	3082(239); 3086(306)
$\nu_{10}(a'')$	HNH bend	1639(46)	1601(0); 1624(164)
$\nu_{11}(a'')$	NH_2 twist	1193(23)	1285(185); 1270(99)
$\nu_{12}(a'')$	HONH torsion	318(161)	804(14); 789(110)
		NO_3^-	
$\nu_1(a')$	NO symm. stretch	1066(0)	1044(149); 1037(20)
$\nu_2(a'')$	N out-of-plane bend	835(8)	830(0); 827(67)
$\nu_3(e'')$	NO asymm. stretch	1378(602)	1483(72),1311(410); 1517(867),1306(115)
$\nu_4(e'')$	ONO bend	709(0)	729(3),704(3); 727(4),702(27)

[a]Labels are assigned to the molecules in their free form.
[b]The frequencies of $HONH_3^+$ and NO_3^- moieties is ionic $(HAN)_2$. The frequencies before the semicolon have a' symmetry, while those after the semicolon have a'' symmetry.

structure are compared to those for isolated NH_4^+ and $HONH_3^-$ in Table IV. The greatest changes in going from free $HONH_3^-$ to the $HONH_3^-$ moiety in $(HAN)_2$ are in the lengths of the hydrogen-bonded N–H, which increase from 1.031 Å to 1.058 Å in $(HAN)_2$ IV, and in the bond angle ∠NOH, which decreases from 107.7° to 100.6°. The binding energy of $(HAN)_2$ given in Table III is 43.4 kcal/mol, which is considerably larger than twice the binding energy of the single HAN molecule (12.7 kcal/mol). This is due to the larger electrostatic interactions in the dimer. The harmonic vibrational frequencies of the $(HAN)_2$ structure III are given in Table V and compared to those calculated for isolated NO_3^- and $HONH_3^+$ ions. The greatest shifts are in the frequencies of the hydrogen-bonded protons. The OH stretch frequency decreases by approximately 400 cm^{-1} in the $(HAN)_2$ structure relative to the free ion. The NH stretch frequencies show decreases of 350 to 400 cm^{-1} in the dimer. The HONH torsional vibration, on the other hand, shows an increase of about 500 cm^{-1} in the dimer relative to free $HONH_3^+$.

The $(HAN)_2$ structure V is shown in Fig. 2(b). Compared to structure IV, this structure has a smaller number of hydrogen bonds and no ionic interactions, resulting in a binding energy of only 23.1 kcal/mol, which is less than the ionic form (see Table III).

The ionic form of a single molecular unit of HAN is not

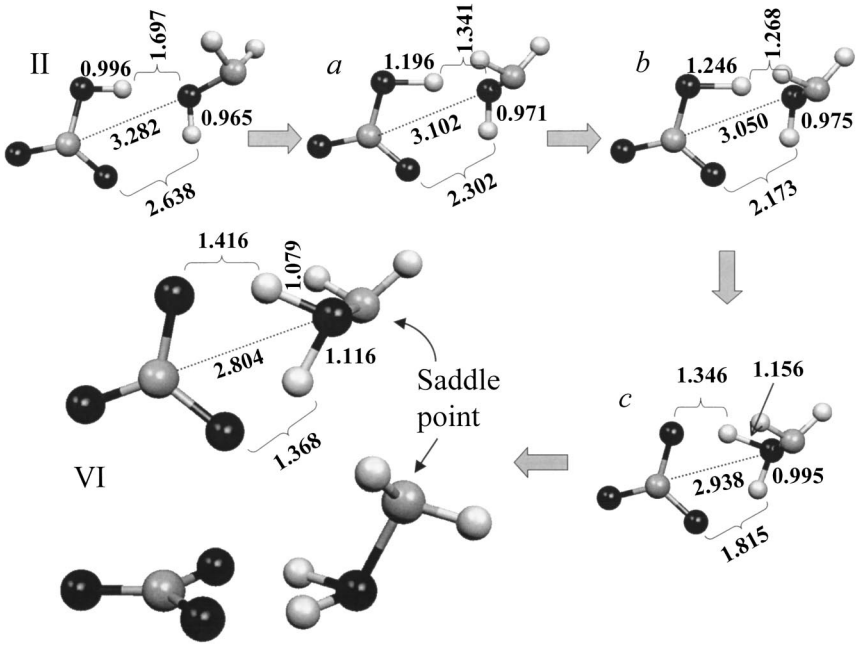

FIG. 3. Stages of the proton exchange reaction from structure II to the ionic saddle-point structure VI. Two views of the saddle-point structure are shown. In structures *a*, *b*, and *c*, the length of the O1–H1 bond is extended relative to II. Note that the saddle point is not symmetric with respect to the O1–H1 (1.416 Å) and O2–H4 (1.368 Å) distances and the torsional angle of the NH_2 group. Selected bond lengths (Å) are shown in the figure and the energies of the configurations are given in Fig. 4.

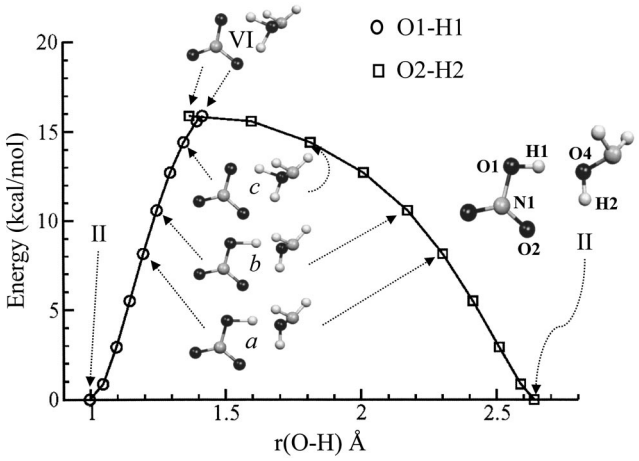

FIG. 4. The energy profile for the proton exchange reaction of structure II of HAN as a function of the O1–H1 (circles) and O2–H2 (squares) distances. The labels O1, H1, O2, H2, and O4 are shown on structure II. Bond lengths of structures II, *a*, *b*, *c*, and VI are shown in Fig. 3.

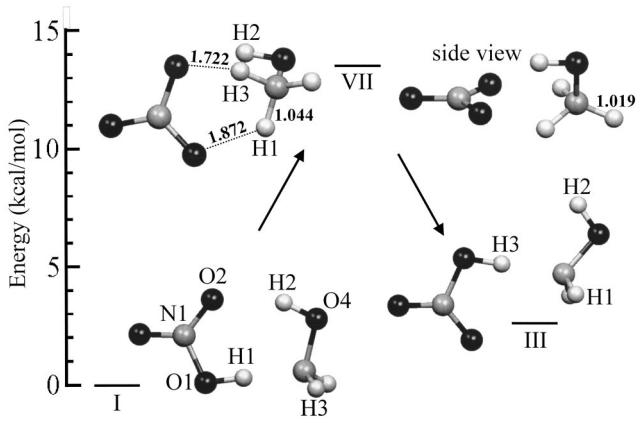

FIG. 5. Starting structures and the saddle point for the proton transfer reaction which converts the HAN I isomer to HAN III. The saddle point is labeled as HAN VII. The result of this process is that proton H1 of the nitric acid fragment of HAN I is exchanged with H3 of the hydroxylamine fragment.

stable relative to the neutral form. Starting from structure II, a proton exchange reaction similar to that observed in ammonium nitrate can be initiated by increasing the nitric acid O–H bond length (the O1–H1 bond of Fig. 1) and optimizing the structure of the remaining parts of the HAN molecule.[9] Several structures with lengthened nitric acid O1–H1 bonds are shown as *a*, *b*, and *c* in Fig. 3. It can be observed that as the O1–H1 bond length is increased, the O2–H2 and N1–O4 lengths will decrease. The saddle point for the proton exchange, structure VI, is shown in two views and can be considered as one ionic form of HAN. The energy profiles of the proton exchange reaction as a function of the O1–H1 and O2–H2 distances are shown in Fig. 4. As $r(\mathrm{O1-H1})$ is increased from 0.996 Å in structure II to 1.416

TABLE VI. Hydrogen bond lengths (Å) for the three configurations of HAN, calculated at the B3LYP/6-311++G(d,p) level. ionic $(\mathrm{HAN})_2$, neutral $(\mathrm{HAN})_2$, and also various clusters of ammonium nitrate, calculated at the B3LYP/6-311++G(d,p) level. Data from Alavi and Thompson, Ref. 9. (AN) and ammonium dinitramide, calculated at the B3LYP/6-311G(d,p) level. Data from Alavi and Thompson, Ref. 10, (ADN).

Species[a]		$R_{\mathrm{A-H}}^{\mathrm{complex}}$	$R_{\mathrm{A-H}}^{\mathrm{isolated}}$	$R_{\mathrm{B-H}}^{\mathrm{complex}}$	$R_{\mathrm{B-H^+}}^{\mathrm{isolated}}$
I-HAN	(O–H···N)	1.029	0.971	1.652	1.031
	(O–H···O)	0.971	0.961	1.968	0.971
II-HAN	(O–H···O)	0.996	0.971	1.697	0.981
	(O–H···O)	0.965	0.961	2.635	0.971
III-HAN	(O–H···N)	1.017	0.971	1.699	1.031
	(N–H···O)	1.019	1.016	3.013	0.971
IV-$(\mathrm{HAN})_2$ (ionic)	(O–H···O)	0.994	0.975	1.746	0.972
	(N–H···O)	1.057	1.031	1.702	0.972
	(N–H···O)	1.046	1.031	1.811	0.972
V-$(\mathrm{HAN})_2$ (molecular)	(O–H···O)	1.019	1.019	2.420	0.971
	(N–H···O)	1.009	0.971	1.623	0.981
AN	(O–H···N)	1.025	0.971	1.664	1.026
	(N–H···O)	1.017	1.014	1.705	0.971
$(\mathrm{AN})_2$	(N–H···O)	1.057	1.026	1.705	0.971
$(\mathrm{AN})\mathrm{HNO_3}$	(N–H···O)	1.107	1.026	1.493	0.971
	(N–H···O)	1.032	1.026	1.877	0.971
	(O–H···O)	1.020	0.971	1.550	0.971
$(\mathrm{AN})\mathrm{NH_3}$	(N–H···N)	1.031	1.014	2.051	1.026
	(N–H···O)	1.018	1.014	2.261	0.971
	(O–H···N)	1.066	0.971	1.535	1.026
ADN-I	(N–H···N)	1.066	1.018	1.736	1.026
ADN-IIb	(O–H···N)	1.041	0.972	1.592	1.026
	(N–H···O)	1.017	1.018	2.600	0.972
ADN-IIc	(O–H···N)	1.046	0.972	1.574	1.026
	(N–H···O)	1.017	1.018	2.614	0.972
$(\mathrm{ADN})\mathrm{NH_3}$	(N–H···N)	1.079	1.026	1.666	1.018
	(N–H···N)	1.072	1.026	1.957	1.026
$(\mathrm{ADN})_2$	(N–H···N)	1.061	1.026	1.744	1.108

[a]Labels refer to structures shown in Figs. 1 and 2.

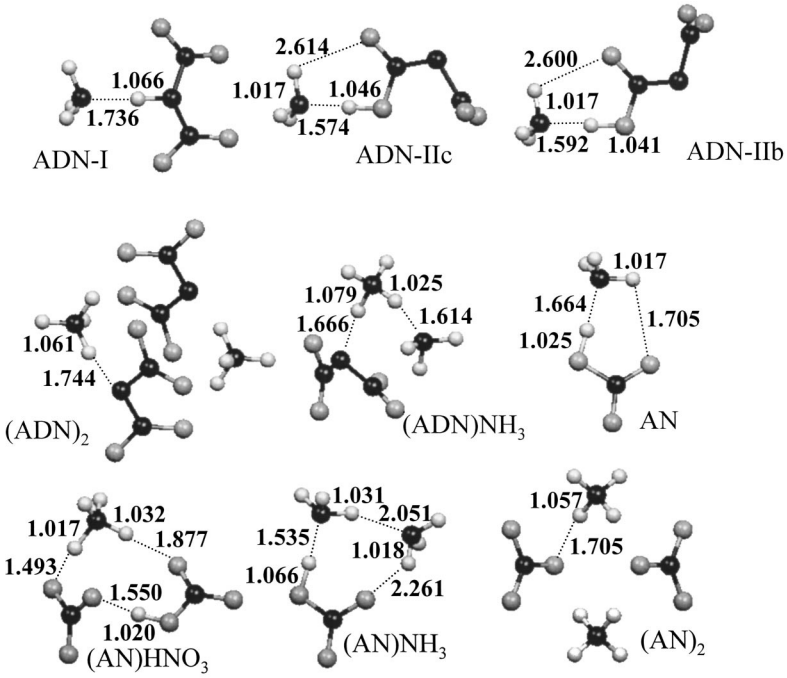

FIG. 6. Ammonium dinitramide (ADN) and ammonium nitrate (AN) species used to study the hydrogen-bond correlation relation of Eq. (3). Hydrogen-bond lengths (Å) are indicated. The AN results are from Alavi and Thompson (Ref. 9).

Å in structure VI, the energy of the complex increases. The dependence of the energy of the molecule on the $r(\mathrm{O1}-\mathrm{H1})$ distance is shown with circles in Fig. 4. This same process can be described in terms of a decrease in the $r(\mathrm{O2}-\mathrm{H2})$ length on going from structure II to VI. The change of energy with decreasing $r(\mathrm{O2}-\mathrm{H2})$ is shown by the squares in Fig. 4. Because of the orientation of the NH_2 group, the transition state is not symmetric and $r(\mathrm{O1}-\mathrm{H1})$ differs from $r(\mathrm{O2}-\mathrm{H2})$ at the transition state.

Unlike the symmetric proton exchange process in ammonium nitrate,[9] the two protons exchanged in the saddle-point structure VI (H1 and H2) are not equivalent. In the stable configuration of hydroxylamine, the hydrogens on the $-NH_2$ group are initially *trans* to the OH bond. Prior to reaching the saddle point in proton transfer, these NH_2 hydrogens retain their general direction opposed to the hydroxylamine OH bond. This is illustrated by the structures given in Fig. 3. However, as the OH proton migrates towards nitric acid and the proton of nitric acid migrates towards hydroxylamine, the $-NH_2$ group must rotate to remain *trans* with respect to the shortest OH bond. Simultaneously, as the two protons are exchanged on the oxygen atom of hydroxylamine, the oxygen end of the hydroxylamine moves closer to the nitric acid. This change in the N1–O4 distance is seen in Fig. 3. A similar change is observed in the distance between ammonium and nitrate N atoms in ammonium nitrate proton transfer.[9] The proton transfer in HAN is thus accompanied by two large rearrangements of heavy-atom groups, the rearrangement of the hydroxylamine towards nitric acid and the rotation of the NH_2 group. These reorientations are seen in Fig. 3.

A proton exchange pathway also exists which converts the HAN I configuration to HAN III. The saddle point for this proton transfer reaction is labeled as VII in Fig. 5. As the nitric acid proton in HAN I is transferred to the lone pair of the hydroxylamine nitrogen, the hydroxylamine undergoes a rotation which brings two of the hydroxylamine NH bonds to a configuration across from the nitric acid oxygens (see HAN VII in Fig. 5). The transfer of the proton of the second of these HN bonds to the nitrate group and a further motion of the OH segment in HAN VII away from the nitric acid molecule leads to the formation of the HAN III isomer. Again, an ionic form of HAN (i.e., HAN VII) is a saddle point in the proton transfer pathway of two stable hydrogen-bonded HAN structures. A proton transfer in HAN I, without change in the orientation of the hydroxylamine moiety, does not occur as it would lead to an unstable zwitterionic form of hydroxylamine ($^{+}H_3NO^{-}$).

IV. DISCUSSION

In the bond-valence model[30] the bond length R_{ij} between atoms i and j and the bond valence s_{ij} are related by Pauling's exponential model function[30,31]

$$s_{ij}=\exp\left(\frac{R_{ij}^{0}-R_{ij}}{b}\right), \tag{1}$$

where R_{ij}^{0} is the length of the bond at unit valence and b is a constant equal to 0.37 Å. According to this model, the total valence of the bonds to a hydrogen atom in A–H···B is 1

$$s_{\mathrm{H-A}}+s_{\mathrm{H-B}}=1. \tag{2}$$

Steiner[32] and Alkorta and Elguero[33,34] have applied this relation to bond lengths in hydrogen-bonded acid–base systems A···H···B, where HA is the acid and B the base group participating in the hydrogen bonding. Alkorta and Elguero define $R_1=R_{\mathrm{A}\cdots\mathrm{H}}^{\mathrm{complex}}-R_{\mathrm{A-H}}^{\mathrm{isolated}}$ and $R_2=R_{\mathrm{B}\cdots\mathrm{H}}^{\mathrm{complex}}-R_{\mathrm{B-H+}}^{\mathrm{isolated}}$. Using these definitions in Eq. (1) and substituting into Eq. (2), the relation

$$(R_1+R_2)=(R_1-R_2)+2b\ln\{1+\exp[-(R_1-R_2)/b]\} \tag{3}$$

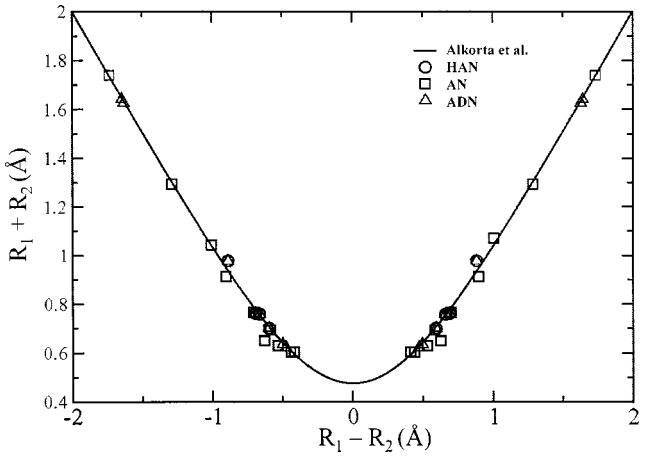

FIG. 7. A plot of (R_1+R_2) as a function of (R_1-R_2) for HAN calculated in this work, AN (Ref. 9) and ADN (Ref. 10) and their clusters, and a comparison with the correlation of Alkorta *et al.* (Ref. 34) from Eq. (3) with $b=0.343$.

between the bond lengths is obtained. Alkorta and Elguero tested this relation extensively with experimental and theoretical bond lengths for neutral and negatively charged basic groups such as SCN^-, OCN^-, substituted amines, phosphenes, and ethers, with hydrogen halides as the acid components. By fitting the data for hydrogen bonds to Eq. (3), a value of $b=0.343\pm0.004$ was obtained with a correlation factor, r^2, greater than 0.985. Steiner[32,35] tested a different form of this correlation with neutron diffraction data for a wide variety of hydrogen bond types including N–H···O, O–H···N, O–H···S, N–H···S, N–H···Cl^-, O–H···O, and C–H···O and also obtained good correlations.

In the present work, we extend the application of Eq. (3) to the hydrogen-bonded HAN, ammonium nitrate,[9] and ammonium dinitramide[10] clusters; a list of the species considered is given in Table VI. The types of hydrogen bonds in these systems include O–H···N, N–H···N, O–H···O, $^+$N–H···O^-, and $^+$N–H···N^-. In gas-phase clusters such as the $(HAN)_2$ complex shown in Fig. 2, there is more than one type of hydrogen bond. The strengths of these hydrogen bonds differ based on the donor and acceptor atoms and also the geometric arrangement of the bonds.

The hydrogen-bonded molecules, other than those calculated in this work, are shown in Fig. 6. The various bond lengths used are given in Table VI and the agreement with Eq. (3) is shown in Fig. 7. The data points are plotted along with the correlation of Alkorta and Elguero[33] with $b=0.343$, and the agreement is seen to be very good. Considering the various types of hydrogen bonding in the complexes of Table VI, it is seen that Eq. (3) quite accurately describes the bond lengths of these hydrogen-bonded systems.

V. SUMMARY AND CONCLUSIONS

Structures, vibrational frequencies, and binding energies of gas-phase hydroxylamine nitrate molecules and dimers are determined in this work. As in many other cases involving ammonium or substituted ammonium salts,[11] proton transfer does not occur in the isolated gas-phase molecule. Due to the presence of two basic atoms on hydroxylamine, the three stable hydrogen-bonded structures I, II, and III are found for the HAN molecule. The ionic form for the more stable HAN I configuration is an unstable zwitterion and the ionic forms HAN VI and HAN VII are saddle points for proton exchange between nitric acid and the hydroxylamine oxygen.

Two stable structures were also found for $(HAN)_2$. The more stable of the two structures, IV, is ionic and has a binding energy which is approximately 50% larger than the neutral hydrogen-bonding structure V. The molecular configurations in IV allow three hydrogen-bonding interactions for each hydroxylammonium ion, whereas the less stable structure V has only two hydrogen-bonding interactions.

A correlation for hydrogen-bond lengths based on the bond valence model was tested for the stable HAN and $(HAN)_2$ molecules. These bond lengths fit the bond length correlation scheme of Alkorta *et al.*[33] very well.

ACKNOWLEDGMENT

This work was supported by AFOSR (Grant Number F49620-00-1-0273).

[1] For a succinct discussion of ammonium perchlorate decomposition, see, T. B. Brill and B. T. Budenz, in *Solid Propellant Chemistry, Combustion, and Motor Interior Ballistics*, Progress in Astronautics and Aeronautics, Vol. 185, edited by V. Yang, T. B. Brill, and W.-Z. Ren (2000), pp. 3–32; see also references therein.
[2] A. K. Galwey and M. E. Brown, *Thermal Decomposition of Ionic Solids* (Elsevier, Amsterdam, 1999).
[3] D. C. Sorescu and D. L. Thompson, J. Phys. Chem. A **105**, 720 (2001).
[4] M. J. Rossi, J. C. Bottaro, and D. F. McMillen, Int. J. Chem. Kinet. **25**, 549 (1993).
[5] S. Alavi and D. L. Thompson, J. Chem. Phys. **119**, 232 (2003).
[6] D. C. Sorescu and D. L. Thompson, J. Phys. Chem. B **103**, 6774 (1999).
[7] D. C. Sorescu and D. L. Thompson, J. Phys. Chem. A **105**, 7413 (2001).
[8] G. F. Velardez, S. Alavi, and D. L. Thompson, J. Chem. Phys. (to be published).
[9] S. Alavi and D. L. Thompson, J. Chem. Phys. **117**, 2599 (2002).
[10] S. Alavi and D. L. Thompson, J. Chem. Phys. **118**, 2599 (2003).
[11] R. A. Cazar, A. J. Jamka, and F.-M. Tao, J. Phys. Chem. A **102**, 5117 (1998); M. Meuwly, A. Bach, and S. Leutwyler, J. Am. Chem. Soc. **123**, 11446 (2001); M. Meuwly and M. Karplus, J. Chem. Phys. **116**, 2572 (2002); J. A. Snyder, R. A. Cazar, A. J. Jamka, and F.-M. Tao, J. Phys. Chem. A **103**, 7719 (1999); A. C. Legon and C. A. Rego, J. Chem. Phys. **90**, 6867 (1989); A. C. Legon, A. L. Wallwork, and C. A. Rego, J. Chem. Phys. **92**, 6397 (1990); A. C. Legon and C. A. Rego, *ibid.* **99**, 1463 (1993); T. Asada, H. Haraguchi, and K. Kitaura, J. Phys. Chem. **105**, 7423 (2001); S. Ikuta, J. Chem. Phys. **87**, 1900 (1987); A. Fernández-Ramos, Z. Smedarchina, W. Siebrand, and M. Z. Zgierski, *ibid.* **113**, 9714 (2000); F.-M. Tao, *ibid.* **108**, 193 (1998); P. Pagsberg, E. Ratajczak, A. Sillesen, and Z. Latajka, Chem. Phys. Lett. **227**, 6 (1994); I. Alkorta, I. Rozas, O. Mó, M. Yáñez, and J. Elguero, J. Phys. Chem. A **105**, 7481 (2001).
[12] S. Tsunekawa, J. Phys. Soc. Jpn. **33**, 167 (1972).
[13] D. Luckhaus, J. Chem. Phys. **106**, 8409 (1997).
[14] L. Rheingold, J. T. Cronin, T. B. Brill, and F. K. Ross, Acta Crystallogr., Sect. C: Cryst. Struct. Commun. **C43**, 402 (1987).
[15] J. T. Cronin and T. B. Brill, J. Phys. Chem. **90**, 178 (1986).
[16] N. Klein, 27th JANNAF Combustion Subcommittee Meeting CPIA Pub. 557, Vol. 1, 443 (1990).
[17] N. Klein, BRL-TR-2641, Ballistic Research Laboratory, Aberdeen Proving Ground, MD, Feb. 1985.
[18] M. J. Frisch, G. W. Trucks, H. B. Schlegel *et al.*, GAUSSIAN 98, Revision A.7, Gaussian, Inc., Pittsburgh, PA, 2001.
[19] A. D. Becke, J. Chem. Phys. **98**, 5648 (1993).
[20] W. Koch and M. C. Holthausen, *A Chemist's View of Density Functional Theory* (Wiley-VCH, Weinheim, 2000).
[21] I. N. Levine, *Quantum Chemistry* (Prentice-Hall, Englewood Cliffs, NJ, 1991).

[22] F.-M. Tao, Int. Rev. Phys. Chem. **20**, 617 (2001).
[23] S. F. Boys and F. Bernardi, Chem. Phys. **232**, 299 (1970).
[24] S. S. Xantheas, J. Chem. Phys. **104**, 8821 (1996).
[25] M.-T. Nguyen, A. J. Jamka, R. A. Cazar, and F.-M. Tao, J. Chem. Phys. **106**, 8710 (1997).
[26] A. K. Chandra and M. T. Nguyen, Chem. Phys. **232**, 299 (1998).
[27] J. M. Molina, J. A. Dobado, M. C. Daza, and J. L. Villaveces, J. Mol. Struct.: THEOCHEM **580**, 117 (2002).
[28] A. P. Cox and J. M. Riveros, J. Chem. Phys. **42**, 3106 (1965).
[29] G. E. McGraw, D. L. Bernitt, and I. C. Hisatsune, J. Chem. Phys. **42**, 237 (1965); A. Perrin, O. Lado-Bordowsky, and A. Valentini, Mol. Phys. **67**, 249 (1989); A. Goldman, J. B. Burkholder, C. J. Howard, R. Escribano, and A. G. Maki, J. Mol. Spectrosc. **131**, 195 (1988); A. G. Maki and W. B. Olson, *ibid.* **133**, 171 (1989).
[30] I. D. Brown, Acta Crystallogr., Sect. B: Struct. Sci. **B48**, 553 (1992).
[31] L. Pauling, J. Am. Chem. Soc. **69**, 542 (1947).
[32] T. Steiner, J. Phys. Chem. A **102**, 7041 (1998).
[33] I. Alkorta and J. Elguero, Struct. Chem. **10**, 157 (1999).
[34] I. Alkorta, I. Rozas, O. Mó, M. Yánez, and J. Elguero, J. Phys. Chem. A **105**, 7481 (2001).
[35] G. R. Desiraju and T. Steiner, *The Weak Hydrogen Bond* (Oxford University Press, Oxford, 2001).